Citation: BoneKEy Reports **5**, Article number: 778 (2016) | doi:10.1038/bonekey.2016.5

www.nature.com/bonekey

ORIGINAL ARTICLE

Activation of intracellular calcium signaling in osteoblasts colocalizes with the formation of post-yield diffuse microdamage in bone matrix

Hyungjin Jung[1] and Ozan Akkus[1,2,3]

[1]Department of Mechanical and Aerospace Engineering, Case Western Reserve University, Cleveland, OH, USA. [2]Department of Orthopedics, Case Western Reserve University, Cleveland, OH, USA. [3]Department of Biomedical Engineering, Case Western Reserve University, Cleveland, OH, USA.

Previous studies demonstrated that extracellular calcium efflux ($[Ca^{2+}]_E$) originates from the regions of bone extracellular matrix that are undergoing microdamage. Such $[Ca^{2+}]_E$ is reported to induce the activation of intracellular calcium signaling ($[Ca^{2+}]_I$) in MC3T3-E1 cells. The current study investigated the association between microdamage and local activation of intracellular calcium signaling quantifiably in MC3T3-E1 cells. Cells were seeded on devitalized notched bovine bone samples to induce damage controllably within the field of observation. A sequential staining procedure was implemented to stain for intracellular calcium activation followed by staining for microdamage on the same sample. The increase in $[Ca^{2+}]_I$ fluorescence in cells of mechanically loaded samples was greater than that of unloaded negative control cells. The results showed that more than 80% of the cells with increased $[Ca^{2+}]_I$ fluorescence were located within the damage zone. In conclusion, the findings demonstrate that there are spatial proximity between diffuse microdamage induction and the activation of intracellular calcium ($[Ca^{2+}]_I$) signaling in MC3T3-E1 cells. The downstream responses to the observed activation in future research may help understand how bone cells repair microdamage.

BoneKEy Reports **5**, Article number: 778 (2016) | doi:10.1038/bonekey.2016.5

Introduction

Fatigue associated with daily activities or overload episodes may induce microdamage in bone matrix.[1–3] Such critically loaded regions of bone are resorbed by osteoclasts and replaced by new bone matrix via the action of osteoblasts.[4] Microdamage in bone is categorized as linear microcracks and diffuse microdamage.[5] Linear microcracks are mesoscale frank ruptures in bone's matrix.[6] Such cracks are reported to induce osteocyte apoptosis by disrupting osteocyte network, which in turn may trigger local repair response through the activation of osteoclasts.[7] On the other hand, diffuse microdamage[8,9], which is defined as clouds of submicron cracks, does not appear to affect osteocyte integrity.[5] The repair response to diffuse damage is likely to take place by alternative mechanisms and likely without the resorption of damaged matrix.[9]

Existing theories on how bone cells respond to mechanical damage involve the effects of increased matrix strain[10–12] or altered fluid flow.[13–16] An emerging theory is that mechanochemical stimulus can activate repair response by osteoblasts.[17] Ion-selective microelectrode measurements have shown calcium efflux from regions of bone undergoing diffuse microdamage to the pericellular space.[17] Such efflux increases the extracellular calcium concentration and depolarizes voltage-gated calcium channels, resulting in the entry of calcium ions from the extracellular niche to the intracellular space ($[Ca^{2+}]_I$) in osteoblasts.[17–19] We have defined this effect as extracellular calcium-induced intracellular calcium response.[18,19] These findings suggest bone matrix as a mechanochemical transducer, which converts mechanical damage stimulus into a chemical signal to trigger cell response. This study aimed to build on this past knowledge by demonstrating the spatial proximity between mechanically induced damage and the activation of $[Ca^{2+}]_I$ signaling in MC3T3-E1 preosteoblasts. Cells were seeded on notched bone samples for spatially controlled induction of damage, and the activation of calcium fluorescence was investigated in registration with the labeling of diffuse damage. In addition to the investigation of cells subjected to microdamage, an unloaded control group and a mechanically loaded group that is far-field to the damage zone were included in the study.

Correspondence: Professor O Akkus, Mechanical and Aerospace Engineering, Case Western Reserve University, 10900 Euclid Avenue, Cleveland, OH 44106, USA. E-mail: oxa@case.edu

Received 5 August 2015; accepted 6 January 2016; published online 2 March 2016

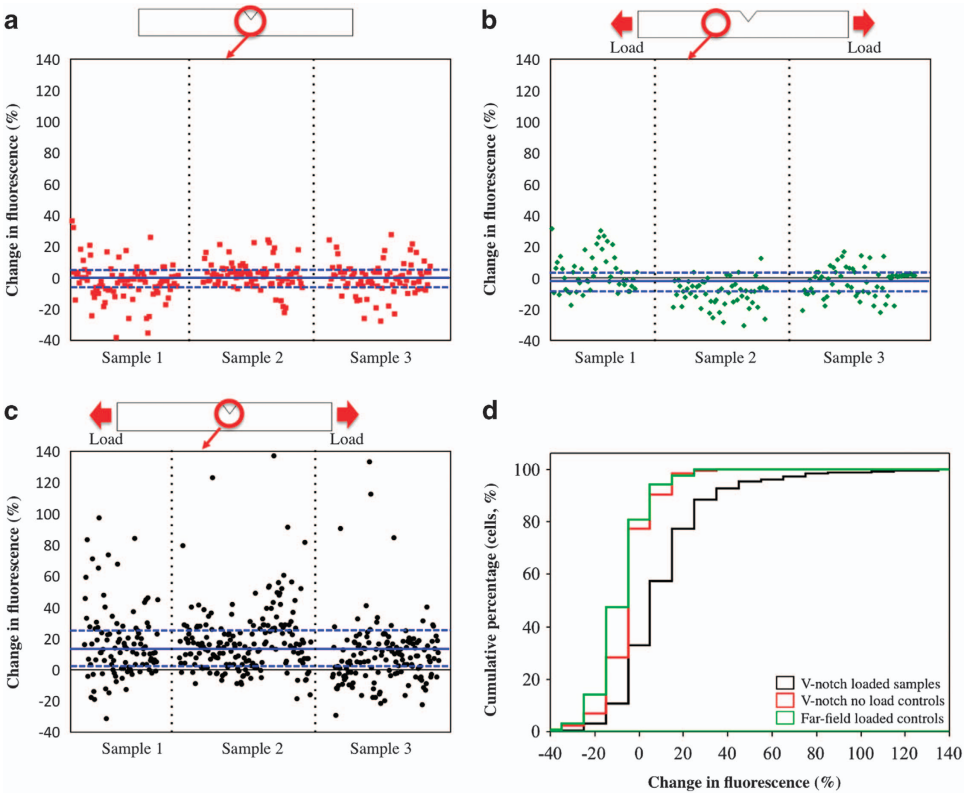

Figure 1 Changes in intracellular calcium fluorescence following mechanically induced matrix damage. Percent changes in fluorescence for individual cells from three specimens are pooled in these plots. (**a**) Negative control cells in the notched region that were not loaded, (**b**) cells outside the damage zone of mechanically loaded samples, (**c**) Response of cells in the damage zone of mechanically loaded samples. The lines highlight the upper quartile, median and lower quartile from top to the bottom. Cells that demonstrated more than 5% increase in fluorescence were classified as activated. (**d**) Cumulative histogram of all three results demonstrates that there is a shift to increased levels of intracellular calcium fluorescence (*x* axis) with damage induction. (Blue line on the image represents Q1, median and Q3, respectively.)

Results

Basal variations of $[Ca^{2+}]_I$ in the absence of mechanical damage and determination of the threshold for calcium activation

The basal variation in $[Ca^{2+}]_I$ fluorescence from samples that were not loaded mechanically displayed between -5.2% and $+3.4\%$ (**Figure 1**, **Table 1**). On the basis of this, background fluctuations in $[Ca^{2+}]_I$ fluorescence in the absence of any effectors were estimated as 5%, because selection of the higher value as the threshold is a safer choice to eliminate inclusion of cells whose intracellular calcium levels are varying at basal levels. Therefore, the cells that displayed greater than 5% increase in $[Ca^{2+}]_I$ fluorescence were accepted to be activated.

Percent change in $[Ca^{2+}]_I$ fluorescence in activated cells

Percent change in $[Ca^{2+}]_I$ fluorescence of activated cells that were located in the damage zone of loaded samples was significantly greater than the far-field loaded group and damage zone of the no-load group (**Figure 1**, **Table 1**, $P<0.0001$).

Association between $[Ca^{2+}]_I$ increase in the cell and damaged area under mechanical loading

Cells with increased $[Ca^{2+}]_I$ fluorescence were closely associated with the calcein blue-stained damage zone (**Figure 2**). In all of the three samples tested, more than 80% of activated cells were located within the calcein blue-stained damage zone (**Table 2**).

Table 1 Fluorescence changes in the cells of three groups (%)

	Q1	*Median*	*Q3*	
V-notch loaded sample	1.5	12.1	23.4	
V-notch no-load controls	−5.2	0	3.4	($P<0.0001$)
Far-field loaded controls	−10	−4	2.9	($P<0.0001$)

Discussion

In this paper, the spatial proximity between mechanically induced diffuse microdamage and activation of $[Ca^{2+}]_I$ signaling in cells local to microdamage was evaluated. Unlike Fluo-4AM, which is a live-cell strain, calcein blue may compromise cell viability. Therefore, calcein blue was applied as the second stain after the $[Ca^{2+}]_I$ was obtained. The presented approach enabled more clear analysis of damage and intracellular calcium events than earlier reports.[17,19]

Although osteocytes are more commonly implicated to be involved in responding to matrix damage,[20,21] the study focused on preosteoblasts. Outer envelopes of bones experience higher stresses due to bending or torsion; therefore, osteoblasts are also likely to be in the vicinity of microdamage and likely to be involved to damage stimulus. The effects of diffuse damage on osteocytes were investigated[5,9,22] in prior literature; however, the effects of diffuse damage on osteoblasts are poorly understood.

Under mechanical loading, the samples can be exposed to different types of mechanical stimuli besides mechanically induced $[Ca^{2+}]_E$, such as direct mechanical stretch or fluid shear. So as to assess the potential role of substrate deformations, previous research employed mechanically loaded notched demineralized bone samples that not only lack matrix calcium but also undergo substantially greater levels of matrix deformation than bone specimens.[17] Despite high levels of deformation, it was observed that the intracellular calcium signaling of cells was not activated on demineralized bone specimens, indicating that damage-related calcium release from bone matrix overrides substrate strain in activating the intracellular calcium signaling. So as to further supplement the past research, we employed a control group in which cells located far-field to the notched region to assess whether substrate strain was responsible for intracellular calcium activation. The absence of response in this group affirms that substrate strain or fluid shear did not have a significant role in terms of stimulating intracellular calcium response in our experimental set up.

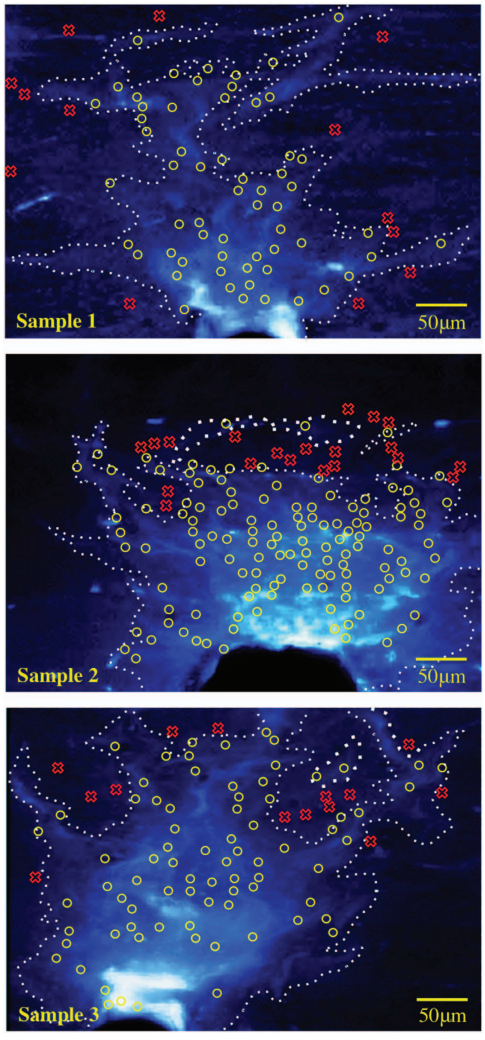

Figure 2 Spatial proximity of $[Ca^{2+}]_I$ increase and damage on bone matrix shown for 3 specimens. (Brightly labeled area is the damaged region as labeled by calcein. Yellow 'O': activated cells on the labeled damage. Red 'X': activated cells outside regions labeled for damage).

Previously, it has been shown that calcium efflux occurs from notched regions of bone wafers ($[Ca^{2+}]_E$), which were damaged in the absence of cells.[17] $[Ca^{2+}]_E$ increase was concomitant with the initiation of microdamage formation and that the efflux subsided as soon as the samples were unloaded. When these experiments were carried out in the presence of cells, $[Ca^{2+}]_I$ was observed only after the emergence of microdamage on bone matrix under critical loading. Furthermore, when experiments were repeated with demineralized notched samples, $[Ca^{2+}]_I$ was diminished. These observations imply that the initial increase in extracellular calcium concentration is associated with efflux from the damaged matrix.

Earlier studies have shown $[Ca^{2+}]_I$ increase in MC3T3-E1 cells following the elevation of $[Ca^{2+}]_E$ by a controlled diffusion chamber.[18,19] Measurements of membrane potential changes in MC3T3-E1 cells indicated hyperpolarization of the cell membrane by accumulation of calcium ion around the cells, followed by membrane depolarization via the activation of the voltage-activated calcium channels (VGCC).[19] This mechanism of $[Ca^{2+}]_E$-induced activation of VGCC was confirmed by pharmaceutical VGCC-specific inhibitors for MC3T3-E1 cells.

The origins of damage-induced calcium efflux in bone matrix remain to be determined. Various mechanisms can be proposed on the emergence of calcium from bone matrix as a result of microdamage. Induction of microdamage introduces submicroscopic cracks, which in turn increase the effective surface area from which the calcium diffusion is occurring.[23] Calcium that is bound to non-collagenous proteins may also become available by disruption of sacrificial bonds.[24] Another possible mechanism may be interfibrillar sliding. Small angle X-ray scattering studies of bone underloading showed that collagen fibrils stayed at a constant strain after yield, suggesting sliding of mineralized collagen fibril after decoupling from the interfibrillar matrix.[25] Such frictional sliding may result in crystal debris formation, acting as a source of $[Ca^{2+}]_E$ efflux.

In this study, microdamage and intracellular calcium fluorescence images were overlapped and analyzed to evaluate the proximity of $[Ca^{2+}]_I$ increase with matrix damage. It was observed that the cells with increased $[Ca^{2+}]_I$ fluorescence were in the damage process zone highlighted by calcein blue. A number of cells with activated intracellular calcium levels were located in the outer demarcations of the damage process zone.

Table 2 Distribution of cells with increased $[Ca^{2+}]_I$ in and out of the damage zone

	Sample 1	*Sample 2*	*Sample 3*
Total number of cells with increased fluorescence	73	144	92
The fraction of cells with increased fluorescence within the damage zone	60 (82%)	124 (86%)	78 (85%)
The fraction of cells with increased fluorescence out of the damage zone	13 (18%)	20 (14%)	14 (15%)

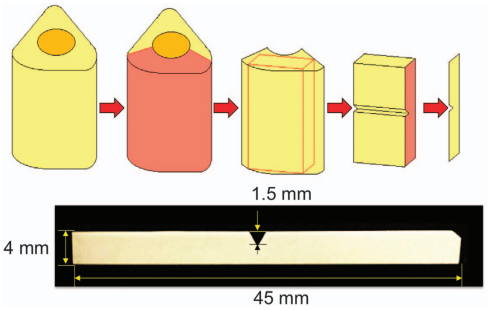

Figure 3 Sample preparation. Bone blocks were prepared from bovine femur, followed by machining of a V-notch in the center of the block. Notched bone blocks were sliced into thin bone wafers (0.2 mm) and polished with 800 and 1200 grade polishing paper and then with 0.3 μm alumina powder.

It is possible that such peripheral cells might be responding to $[Ca^{2+}]_E$ from the nascent microdamage occurring at the fringes of the damage process zone, or the $[Ca^{2+}]_E$ in the damage process may have diffused laterally to activate the cells peripheral to the damage zone. Overall, it is possible that all the activated cells may be associated with damage.

The results showed that not all cells display increased intracellular fluorescence in response to damage. There may be various reasons for that. The first reason may be that the duration of our experiments (90 s) was not long enough to capture late responding cells. For some cells, it may have taken longer than this duration to attain the extracellular calcium threshold sufficient to activate the voltage-gated calcium channels. Another reason for unresponsive cells may be the heterogeneity of the distribution of diffuse damage on bone matrix,[23] such that not every cell may have had damage process taking place in its immediate vicinity. Finally, it is also possible that the sensitivity of cells to extracellular calcium may vary within the cell population. Differences in sensitivities of cells to $[Ca^{2+}]_E$ may induce late or less pronounced $[Ca^{2+}]_I$ response.[26]

Intracellular calcium signaling activates various downstream pathways, some of which may relate to damage repair. It has been reported that increased intracellular calcium levels affect viability, proliferation, differentiation and matrix synthesis by osteoblasts or their progenitors.[27–30] Intracellular calcium activates the synthesis of bone-associated proteins such as OPN, BSN and CaMK2.[31,32] Increased intracellular calcium enhances downstream signaling pathways for Runx2 through the Ras—MAPK pathway.[33,34] Activated Runx2 controls many osteogenic genes through this multicomponent complex, which can interact with the promoter regions of the osteoblast-specific genes such as osteocalcin, osteopontin, collagen I, collagenase 3(matrix metalloproteinase 1), bone sialoprotein alkaline phosphatase (ALP), TGFβ receptor 1 and RANKL (receptor activator of nuclear factor kappa B ligand).[35–40] Osterix, a zinc finger-containing transcription factor, is an osteoblast-specific transcription factor that regulates osteoblast differentiation and mineralization.[41] Calcium activates cox-2,[42] followed by regulation of Osterix levels by cox-2 in osteoblasts.[43] Activated intracellular calcium signaling modulates the Camk-II-Dlx5 pathway, which regulates the Osterix level in osteoblast.[44] Future work will explore the activation of such downstream pathways of intracellular calcium signaling, in association with mechanically induced $[Ca^{2+}]_E$ efflux.

Conclusion

This study confirms spatial proximity between bone matrix damage and intracellular calcium signaling. The results indicate that matrix damage-related chemical alterations in the pericellular space are transduced to the cell as a biological signal. Future studies will focus on downstream pathways of damage repair in response to increased levels of activation of $[Ca^{2+}]_I$ due to microdamage.

Materials and Methods

Chemicals

Minimum essential alpha medium (α-MEM), phenol red-free α-MEM (phenol-free α-MEM), penicillin/streptomycin, trypsin/EDTA, HBSS, HEPES and Fluo-4AM were obtained from Invitrogen (Frederick, MD, USA). Fetal bovine serum (FBS) was purchased from Sigma-Aldrich (St Louis, MO, USA).

Preparation of bone samples

Notched bone wafers were used to introduce damage controllably at a defined location within the field of view. Bovine femurs from ~18-month-old cows were procured from a local butcher in a fresh frozen form. Bone blocks were prepared from bovine femur diaphysis using a milling machine (Series 5400, Sherline, Vista, CA, USA) and a polisher (Buehler Ltd., Lake Bluff, IL, USA; **Figure 3**). A V-notch was introduced in the center of the block using the milling machine and a suitably shaped end mill. Root radius of V-notch was about 50 μm, which was intentionally kept blunt to increase the size of the damage zone. Notched bone blocks were then sliced into thin bone wafers using a low-speed diamond blade saw (Buehler Ltd.) and both surfaces of the wafers were polished with 800 and 1200 grade polishing paper and then with 0.3 μm alumina powder (Buehler Ltd.). After final polishing with alumina powder, samples were sonicated to remove polishing debris. The final dimensions of the wafers were $45 \times 4 \times 0.2$ mm with 1.5 mm depth V-notch in the center. Prior to cell seeding, V-notched bone wafers were kept in 70% ethanol solution overnight for disinfection. Samples were rehydrated in ample amount of sterile phosphate-buffered saline to remove the ethanol prior to cell seeding.

Assessment of $[Ca^{2+}]_I$ activation by mechanically induced $[Ca^{2+}]_E$ efflux

MC3T3-E1 preosteoblasts (ATCC, Manassas, VA, USA, passage 22, sub-clone 4) were used to evaluate the activation of $[Ca^{2+}]_I$ signaling response to damage induction. This cell line was created from C57BL/6 mouse calvaria and differentiated into osteoblasts. Selected sub-clone (sub-clone 4) expressed high levels of alkaline phosphatase and could synthesize mineralized nodules.[45] MC3T3-E1 cells were seeded in monolayer on sterilized V-notched bone wafers at a density of 20,000 cells per cm^2 and cultured overnight with α-MEM supplemented with 10% FBS and 100 U ml^{-1} penicillin/streptomycin, in 37 °C, 5% CO_2.

Changes in cytoplasmic $[Ca^{2+}]_I$ concentration were observed by staining the cell with calcium fluorescent dye, Fluo4-AM (Ex/Em: 494/506 nm). One mM Fluo-4AM was diluted into 5 μM in imaging media (phenol-free α-MEM supplemented with 1% FBS), and cells on the bone slide were incubated in the media with 5 μM Fluo-4AM for 90 min in 37 °C, 5% CO_2. After incubation, cells were washed three times with the imaging media to remove the leftover Fluo-4AM and cultured for an additional 30 min in 37 °C, 5% CO_2, for de-esterification.

Prior research demonstrated the controlled induction of damage using notched bovine bone slices.[23] Briefly, the damage extended to a region of about 0.5×0.5 mm at the notch tip. The damage was discernable as an opaque zone under transmission imaging, and the

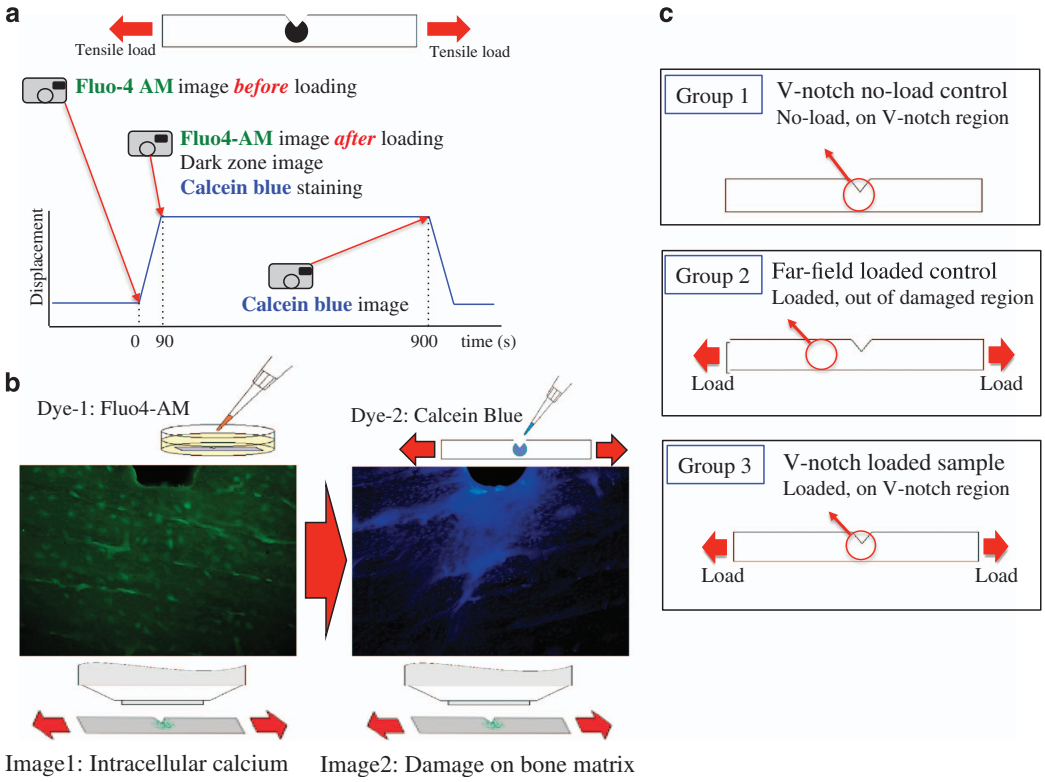

Figure 4 (**a**) Loading history and experimental design for applying stains for sequential imaging of intracellular calcium fluorescence and matrix damage on the same sample. (**b**) Representative images obtained from dual staining. MC3T3-E1 cells were stained with Fluo4-AM for evaluating intracellular calcium signaling, and damage in bone matrix was stained with calcein blue. (**c**) Study groups.

resultant damage was in the form of extensive diffuse microdamage. Cell-seeded notched bone wafers were mounted on a miniaturized tensile test device (Ernest F Fullam, Inc., Albany, NY, USA) fixed on the stage of a light microscope (BX51, Olympus America, Center Valley, PA, USA).

Cells were imaged under three conditions (**Figure 4c**); Group (1): negative control imaging of cells at the notch tip without any loading to record changes in baseline fluorescence over a duration corresponding to the timeline of the experiments, Group (2): away from the notch tip (far-field) under mechanical loading to discern effects of mechanical strain in the underlying bone substrate, Group (3): at the notch tip under mechanical loading to assess damage effects. A threshold of activation was determined by using group 1. There were three specimens in each group.

Bone samples were loaded at 3 $\mu m\,s^{-1}$ using miniaturized tensile test device, which strained the specimens symmetrically from both ends, allowing the point of interest to stay in the same field of view during loading. At this speed, damage zone appeared in about 90 s. A transparent window at the bottom of the device allowed for visualization of the emergence of the damage zone in transmission imaging mode as we had reported before.[23] The loading was stopped upon the emergence of the damage zone to image intracellular calcium response.

UV epifluorescent light source and the calcium imaging system (Incyt-IM, Intracellular Imaging, OH, USA) were used for imaging intracellular calcium signaling of Fluo-4AM-labeled cells. A $\times 10$ water immersion objective lens was used to measure the fluorescence of cells before and after microdamage induction. The size of the measurement region was determined by the field of view of the $\times 5$ microscope objective and it is 0.95×0.7 mm. Percent changes in $[Ca^{2+}]_I$ fluorescence in the loaded groups were evaluated by comparing $[Ca^{2+}]_I$ fluorescence in the cells before loading and after loading. In no-load control, percent changes in $[Ca^{2+}]_I$ fluorescence were obtained by comparing $[Ca^{2+}]_I$ fluorescence in the cells at 0 s and at 90 s after starting imaging. In the absence of damage induction, percent change in $[Ca^{2+}]_I$ fluorescence had a median value of -3.4% due to photobleaching. Therefore, data points were adjusted by 3.4% to account for the effects of photobleaching for all groups.

Immediately after securing the collection of $[Ca^{2+}]_I$ data, 1 mM of calcein blue stain (Ex/Em: 322/445 nm) dissolved in water was applied on the damage zone with the sample in the loaded state for 15 min to label microdamage under ambient conditions. Calcein blue-stained images were recorded with UV epifluorescent light source and the calcium imaging system (Incyt-IM). A $\times 10$ water immersion objective lens was used to measure the fluorescence from the stained damage.

The green fluorescent images of $[Ca^{2+}]_I$ and the blue fluorescent images from exposed calcium on microdamage from bone matrix were overlayed to evaluate the special proximity between mechanically induced $[Ca^{2+}]_E$ efflux and $[Ca^{2+}]_I$ increase in the cell (**Figure 5**).

Data analysis

Change in intracellular calcium fluorescence of cells was recorded before and after mechanical loading by the calcium imaging system (Incyt-IM). Recorded fluorescence values in the cells were measured using ImageJ (NIH, Bethesda, MD, USA). A total of 860 cells from three groups, 245 cells from Group 1, 171 cells from Group 2, and 444 cells from Group 3 were analyzed.

Fluorescence recordings of cells in Group 1 were quantified to find the levels of basal fluorescence in the absence of damage. Percent increase in fluorescence values above these basal levels was accepted as activated cells in groups that were stimulated by damage zone induction. Activated cells were then classified in terms of being in or outside the calcein blue-labeled damage zone, which was $0.33 \pm 0.10\ mm^2$ in size.

Data were not normally distributed according to the Anderson-Darling test (Minitab, State College, PA, USA). Therefore, data are presented in terms of median and quartiles. Also, a non-parametric Kruskal–Wallis

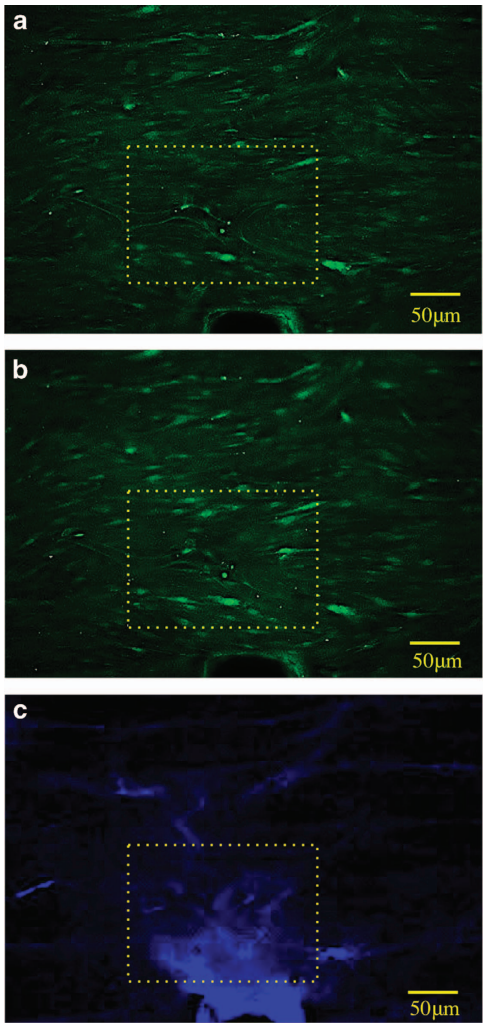

Figure 5 Typical response of intracellular calcium fluorescence before (**a**) and after (**b**) the induction of damage. (**c**) Calcein blue-stained bone matrix damage. Yellow boxes highlight a group of cells that display increased fluorescence after damage induction.

analysis was conducted to test for significant differences. The Mann–Whitney's test was performed to evaluate differences between the loaded group and the control groups, and Bonferroni correction was used for multiple comparisons (Minitab).

Conflict of Interest

The authors declare no conflict of interest.

Acknowledgements

This study was funded by the National Science Foundation under grant number NSF CMMI-1233413. Any opinions, findings, and conclusions or recommendations expressed in this material are those of the authors and do not necessarily reflect the views of the National Science Foundation.

References

1. Zioupos P, Currey JD. The extent of microcracking and the morphology of microcracks in damaged bone. *J Mater Sci* 1994; **29**: 978–986.
2. Reilly GC, Currey JD. The effects of damage and microcracking on the impact strength of bone. *J Biomech* 2000; **33**: 337–343.
3. O'Brien FJ, Taylor D, Lee TC. Microcrack accumulation at different intervals during fatigue testing of compact bone. *J Biomech* 2003; **36**: 973–980.
4. Taylor D, Hazenberg JG, Lee TC. Living with cracks: damage and repair in human bone. *Nat Mater* 2007; **6**: 263–268.
5. Herman BC, Cardoso L, Majeska RJ, Jepsen KJ, Schaffler MB. Activation of bone remodeling after fatigue: differential response to linear microcracks and diffuse damage. *Bone* 2010; **47**: 766–772.
6. Wasserman N, Brydges B, Searles S, Akkus O. In vivo linear microcracks of human femoral cortical bone remain parallel to osteons during aging. *Bone* 2008; **43**: 856–861.
7. Cardoso L, Herman BC, Verborgt O, Laudier D, Majeska RJ, Schaffler MB. Osteocyte apoptosis controls activation of intracortical resorption in response to bone fatigue. *J Bone Miner Res* 2009; **24**: 597–605.
8. Burr DB, Forwood MR, Fyhrie DP, Martin RB, Schaffler MB, Turner CH. Bone microdamage and skeletal fragility in osteoporotic and stress fractures. *J Bone Miner Res* 1997; **12**: 6–15.
9. Seref-Ferlengez Z, Basta-Pljakic J, Kennedy OD, Philemon CJ, Schaffler MB. Structural and mechanical repair of diffuse damage in cortical bone in vivo. *J Bone Miner Res* 2014; **29**: 2537–2544.
10. Yang CM, Chien CS, Yao CC, Hsiao LD, Huang YC, Wu CB. Mechanical strain induces collagenase-3 (MMP-13) expression in MC3T3-E1 osteoblastic cells. *J Biol Chem* 2004; **279**: 22158–22165.
11. Ehrlich PJ, Lanyon LE. Mechanical strain and bone cell function: a review. *Osteoporos Int* 2002; **13**: 688–700.
12. Kreja L, Liedert A, Hasni S, Claes L, Ignatius A. Mechanical regulation of osteoclastic genes in human osteoblasts. *Biochem Biophys Res Commun* 2008; **368**: 582–587.
13. Kapur S, Baylink DJ, Lau KH. Fluid flow shear stress stimulates human osteoblast proliferation and differentiation through multiple interacting and competing signal transduction pathways. *Bone* 2003; **32**: 241–251.
14. Wadhwa S, Godwin SL, Peterson DR, Epstein MA, Raisz LG, Pilbeam CC. Fluid flow induction of cyclo-oxygenase 2 gene expression in osteoblasts is dependent on an extracellular signal-regulated kinase signaling pathway. *J Bone Miner Res* 2002; **17**: 266–274.
15. Tan SD, de Vries TJ, Kuijpers-Jagtman AM, Semeins CM, Everts V, Klein-Nulend J. Osteocytes subjected to fluid flow inhibit osteoclast formation and bone resorption. *Bone* 2007; **41**: 745–751.
16. You J, Reilly GC, Zhen X, Yellowley CE, Chen Q, Donahue HJ *et al.* Osteopontin gene regulation by oscillatory fluid flow via intracellular calcium mobilization and activation of mitogen-activated protein kinase in MC3T3-E1 osteoblasts. *J Biol Chem* 2001; **276**: 13365–13371.
17. Sun X, McLamore E, Kishore V, Fites K, Slipchenko M, Porterfield DM *et al.* Mechanical stretch induced calcium efflux from bone matrix stimulates osteoblasts. *Bone* 2011; **50**: 581–591.
18. Sun X, Kishore V, Fites K, Akkus O. Osteoblasts detect pericellular calcium concentration increase via neomycin-sensitive voltage gated calcium channels. *Bone* 2012; **51**: 860–867.
19. Jung H, Best M, Akkus O. Microdamage induced calcium efflux from bone matrix activates intracellular calcium signaling in osteoblasts via L-type and T-type voltage-gated calcium channels. *Bone* 2015; **76**: 88–96.
20. Noble B. Bone microdamage and cell apoptosis. *Eur Cell Mater* 2003; **6**: 46–55.
21. Heino TJ, Kurata K, Higaki H, Vaananen HK. Evidence for the role of osteocytes in the initiation of targeted remodeling. *Technol Health Care* 2009; **17**: 49–56.
22. Seref-Ferlengez Z, Kennedy OD, Schaffler MB. Bone microdamage, remodeling and bone fragility: how much damage is too much damage[quest]. *BoneKEy Rep* 2015; **4**: 644.
23. Sun X, Hoon Jeon J, Blendell J, Akkus O. Visualization of a phantom post-yield deformation process in cortical bone. *J Biomech* 2010; **43**: 1989–1996.
24. Fantner GE, Hassenkam T, Kindt JH, Weaver JC, Birkedal H, Pechenik L *et al.* Sacrificial bonds and hidden length dissipate energy as mineralized fibrils separate during bone fracture. *Nat Mater* 2005; **4**: 612–616.
25. Gupta HS, Krauss S, Kerschnitzki M, Karunaratne A, Dunlop JW, Barber AH *et al.* Intrafibrillar plasticity through mineral/collagen sliding is the dominant mechanism for the extreme toughness of antler bone. *J Mech Behav Biomed Mater* 2013; **28**: 366–382.
26. Guo L, Davidson RM. Extracellular Ca2 + increases cytosolic free Ca2 + in freshly isolated rat odontoblasts. *J Bone Miner Res* **14**: 1357–1366 1999.
27. Eklou-Kalonji E, Denis I, Lieberherr M, Pointillart A. Effects of extracellular calcium on the proliferation and differentiation of porcine osteoblasts *in vitro*. *Cell Tissue Res* 1998; **292**: 163–171.
28. Yamauchi M, Yamaguchi T, Kaji H, Sugimoto T, Chihara K. Involvement of calcium-sensing receptor in osteoblastic differentiation of mouse MC3T3-E1 cells. *Am J Physiol Endocrinol Metab* 2005; **288**: E608–E616.
29. Nakamura S, Matsumoto T, Sasaki J, Egusa H, Lee KY, Nakano T *et al.* Effect of calcium ion concentrations on osteogenic differentiation and hematopoietic stem cell niche-related protein expression in osteoblasts. *Tissue Eng Part A* 2010; **16**: 2467–2473.
30. Sugimoto T, Kanatani M, Kano J, Kaji H, Tsukamoto T, Yamaguchi T *et al.* Effects of high calcium concentration on the functions and interactions of osteoblastic cells and monocytes and on the formation of osteoclast-like cells. *J Bone Miner Res* 1993; **8**: 1445–1452.
31. Jung GY, Park YJ, Han JS. Effects of HA released calcium ion on osteoblast differentiation. *J Mater Sci Mater Med* 2010; **21**: 1649–1654.
32. Batra NN, Li YJ, Yellowley CE, You L, Malone AM, Kim CH *et al.* Effects of short-term recovery periods on fluid-induced signaling in osteoblastic cells. *J Biomech* 2005; **38**: 1909–1917.
33. Rosen LB, Ginty DD, Weber MJ, Greenberg ME. Membrane depolarization and calcium influx stimulate MEK and MAP kinase via activation of Ras. *Neuron* 1994; **12**: 1207–1221.

34. Kanno T, Takahashi T, Tsujisawa T, Ariyoshi W, Nishihara T. Mechanical stress-mediated Runx2 activation is dependent on Ras/ERK1/2 MAPK signaling in osteoblasts. *J Cell Biochem* 2007; **101**: 1266–1277.
35. Ducy P, Zhang R, Geoffroy V, Ridall AL, Karsenty G. Osf2/Cbfa1: a transcriptional activator of osteoblast differentiation. *Cell* 1997; **89**: 747–754.
36. Selvamurugan N, Chou WY, Pearman AT, Pulumati MR, Partridge NC. Parathyroid hormone regulates the rat collagenase-3 promoter in osteoblastic cells through the cooperative interaction of the activator protein-1 site and the runt domain binding sequence. *J Biol Chem* 1998; **273**: 10647–10657.
37. Kern B, Shen J, Starbuck M, Karsenty G. Cbfa1 contributes to the osteoblast-specific expression of type I collagen genes. *J Biol Chem* 2001; **276**: 7101–7107.
38. Harada H, Tagashira S, Fujiwara M, Ogawa S, Katsumata T, Yamaguchi A *et al.* Cbfa1 isoforms exert functional differences in osteoblast differentiation. *J Biol Chem* 1999; **274**: 6972–6978.
39. Shimizu-Sasaki E, Yamazaki M, Furuyama S, Sugiya H, Sodek J, Ogata Y. Identification of a novel response element in the rat bone sialoprotein (BSP) gene promoter that mediates constitutive and fibroblast growth factor 2-induced expression of BSP. *J Biol Chem* 2001; **276**: 5459–5466.
40. Otto F, Lubbert M, Stock M. Upstream and downstream targets of RUNX proteins. *J Cell Biochem* 2003; **89**: 9–18.
41. Nakashima K, Zhou X, Kunkel G, Zhang Z, Deng JM, Behringer RR *et al.* The novel zinc finger-containing transcription factor osterix is required for osteoblast differentiation and bone formation. *Cell* 2002; **108**: 17–29.
42. Ogata S, Kubota Y, Satoh S, Ito S, Takeuchi H, Ashizuka M *et al.* Ca2 + stimulates COX-2 expression through calcium-sensing receptor in fibroblasts. *Biochem Biophys Res Commun* 2006; **351**: 808–814.
43. Zhang X, Schwarz EM, Young DA, Puzas JE, Rosier RN, O'Keefe RJ. Cyclooxygenase-2 regulates mesenchymal cell differentiation into the osteoblast lineage and is critically involved in bone repair. *J Clin Invest* 2002; **109**: 1405–1415.
44. Samee N, Geoffroy V, Marty C, Schiltz C, Vieux-Rochas M, Levi G *et al.* Dlx5, a positive regulator of osteoblastogenesis, is essential for osteoblast-osteoclast coupling. *Am J Pathol* 2008; **173**: 773–780.
45. Wang D, Christensen K, Chawla K, Xiao G, Krebsbach PH, Franceschi RT. Isolation and characterization of MC3T3-E1 preosteoblast subclones with distinct in vitro and in vivo differentiation/mineralization potential. *J Bone Miner Res* 1999; **14**: 893–903.